

**Supplementary Information for “A length descriptor to
measure the linear and third-order nonlinear optical
responses of atomic-cluster isomers”**

Quanjie Zhong*

School of Materials Science and Physics, China University of Mining and Technology,

Xuzhou 221116, Jiangsu Province, China

E-mail address: quanjiezhong@cumt.edu.cn

Table of Contents

Building the reliable data set	2
Table S1. Assessment for the geometrical optimization and HOMO–LUMO gap calculations of silicon clusters	3
Table S2. Assessment for the geometrical optimization and HOMO–LUMO gap calculations of phosphorus clusters	4
Table S3. Assessment for the geometrical optimization and HOMO–LUMO gap calculations of sulfur clusters	5
Figure S1. FOD calculations of atomic-cluster isomers	7
Figure S2. Assessments for calculating the linear and nonlinear optical responses of silicon, phosphorus, and sulfur isomers.....	9
Optical response behaviors of atomic-cluster isomers	10
Figure S3. Measuring the linear and nonlinear optical responses of atomic clusters using the HOMO–LUMO gap descriptor	11
Figure S4. Measuring the linear and nonlinear optical responses of atomic clusters using the maximum atomic distance descriptor.....	12
Optical response behaviors of 1D geometries	13
Figure S5. Optical responses of the designed Si ₂₀ isomer	13
Figure S6. Optical responses of the acetylene oligomers (<i>trans</i> -configuration)	14
References.....	15

Building the reliable data set

A series of measures were performed to build the reliable data set for analyzing the linear and nonlinear optical responses of atomic clusters. 210 initial isomers of silicon, phosphorus, and sulfur clusters containing n ($n = 20$) atoms were generated by randomly moving atoms, respectively. Initial geometries of atomic-cluster isomers are regulated by controlling atomic allowed coordinate parameters to enlarge the structural diversity. Atomic-cluster isomers were optimized to minima on their adiabatic potential energy surfaces using the PBE0 functional^{1,2} and the def-SVP basis set³. Among them, isomers that do not converge in geometric optimization were abandoned. Then, 202, 205, and 200 optimized isomers of silicon, phosphorus, and sulfur were obtained, respectively. To ensure the reliability of geometric optimization scheme, a series of assessments using the dispersion corrected PBE0 functional (Grimme's DFT-D3 correction with Becke–Johnson damping^{4,5}) in combination with the def2-SVP basis set were performed. Here, the Si₂, Si₆, P₂, P₄, S₂, S₆ clusters containing even-numbered atoms and Si₇, P₃, S₃ containing odd-numbered atoms were selected as the assessment systems owing to their available experimental values. As shown in **Table S1–S3**, the geometrical parameter and vibration frequency of these clusters calculated using the PBE0 functional and def2-SVP basis set are in good agreement with the experimental values. Other functionals such as pure functional PBE,⁶ hybrid functional B3LYP,^{7,8} and double-hybrid functional B2PLYP⁹ also evaluated for accurately calculating geometrical parameter and vibration frequency, the PBE0 functional shows the best robustness. Similar to the case of geometric optimization, the PBE0/def-SVP level was identified to be capable of reasonably evaluating the HOMO–LUMO gap of silicon, phosphorus, and sulfur clusters by comparing the simulated ionization potential with the experimental data reported in the literature.

Table S1. Assessment for the geometrical optimization and HOMO–LUMO gap calculations of silicon clusters. Simulated bond length, vibration frequency, and adiabatic ionization potential with their corresponding experimental values.

cluster	bond length (Å)		vib. fre. (cm ⁻¹)		ion. pot. (eV)	
	exp. ¹⁰	cal.	exp. ^{10–12}	cal.	exp. ^{13,14}	cal.
Si ₂	2.25	2.27	511	511	7.92	8.01
Si ₆			252	249		
			300	325		
			386	405	7.90	7.77
			404	422		
			458	474		
			464	471		
Si ₇			289	277		
			340	336		
			340	337	7.9	7.98
			358	354		
			417	399		
			435	422		

Table S2. Assessment for the geometrical optimization and HOMO–LUMO gap calculations of phosphorus clusters. Simulated bond length, vibration frequency, and adiabatic ionization potential with their corresponding experimental values.

cluster	bond length (Å)		vib. fre. (cm ⁻¹)		ion. pot. (eV)	
	exp. ^{15,16}	cal.	exp. ^{17,18}	cal.	exp. ¹⁹	cal.
P ₂	1.89	1.89	775	833	10.6	10.46
P ₃			460	427	8.09	7.79
			645	650		
P ₄	2.22	2.20	360	392	9.28	9.32
			450	490		
			600	636		

Table S3. Assessment for the geometrical optimization and HOMO–LUMO gap calculations of sulfur clusters. Simulated bond length, vibration frequency, and adiabatic ionization potential with their corresponding experimental values.

cluster	bond length (Å)		vib. fre. (cm ⁻¹)		ion. pot. (eV)	
	exp. ²⁰	cal.	exp. ²¹	cal.	exp. ²²	cal.
S ₂	1.89	1.91	726	744	9.36	9.47
S ₃	1.90	1.93	256	258	9.68	9.68
			575	523		
			656	695		
			180	165		
S ₆	2.07	2.08	203	205	9.00	8.87
			265	272		
			312	321		
			390	352		
			451	445		
			462	469		
			477	492		

Atomic clusters often exhibit multi-reference characteristics, and single-reference theories fail to accurately evaluate the physical and chemical properties of such systems. Here, the fractional occupation number weighted electron density (FOD) analysis was performed to remove systems with significant multi-reference characteristics.²³ In detail, the integration value of the FOD over all space, i.e., N_{FOD} value, is used as a criterion to exclude silicon isomers with N_{FOD} values larger than 3.2, phosphorus isomers with N_{FOD} values larger than 2.2, and sulfur isomers with N_{FOD} values larger than 2.0 (**Figure S1**). A tight standard (i.e., a small N_{FOD} value) leads to few atomic-cluster isomers being remained, while a loose standard (i.e., a large N_{FOD} value) makes it difficult to exclude the systems with significant multi-reference characteristics. Therefore, the determined N_{FOD} value is a compromise. Finally, 151, 169, and 150 eligible isomers of silicon, phosphorus, and sulfur clusters were remained, respectively.

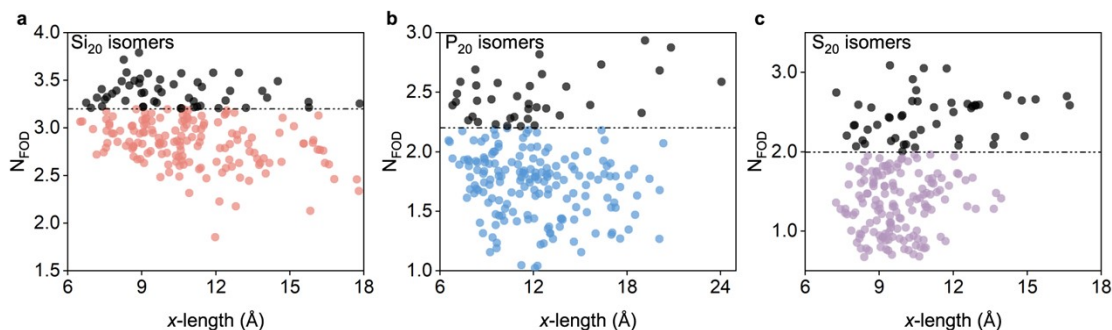


Figure S1. FOD calculations of atomic-cluster isomers. (a) silicon-cluster isomers ($n = 202$), (b) phosphorus-cluster isomers ($n = 205$), and (c) sulfur-cluster isomers ($n = 200$). Black-dashed lines represent the N_{FOD} values with 3.2 for silicon-cluster isomers, 2.2 for phosphorus-cluster isomers, and 2.0 for sulfur-cluster isomers.

Previous studies on organic molecules have indicated that the determination of a reliable exchange-correlation functional to calculate the γ depends on the system being studied.²⁴ Herein, assessments were performed to determine a functional suitable for calculating the α and γ of silicon, phosphorus, and sulfur cluster isomers. Second-order Møller-Plesset (MP2) method is considered as a reliable method for evaluating the nonlinear optical responses.²⁵ Therefore, the α_{xx} and γ_{xxxx} values calculated using various functionals (pure functional PBE, hybrid functional PBE0, and range-separated functional CAM-B3LYP²⁶) paired with aug-cc-pVDZ basis set²⁷ were compared with those of the RIJCOSX-MP2/aug-cc-pVDZ level^{28–34}. As shown in **Figure S2**, the PBE and PBE0 functionals systematically overestimate the evolution trend of the α_{xx} and γ_{xx} values with x -length owing to significant delocalization error. In contrast, the CAM-B3LYP functional perfectly reproduces the evolution trend of the α_{xx} and γ_{xx} values obtained by RIJCOSX-MP2 method with x -length. In particular, the α_{xx} and γ_{xx} values of sulfur clusters calculated using the CAM-B3LYP functional are in good agreement with those of the RIJCOSX-MP2 method. Therefore, the α and γ components were calculated at the CAM-B3LYP/aug-cc-pVDZ level for all atomic cluster isomers. In evaluating functional suitable for calculating the nonlinear optical responses, all selected clusters were not pre-calculated in terms of the α_{xx} and γ_{xx} values, and the unique criterion is the x -length. Up to now, the reliable data set for analyzing the linear and nonlinear optical responses of atomic clusters were established.

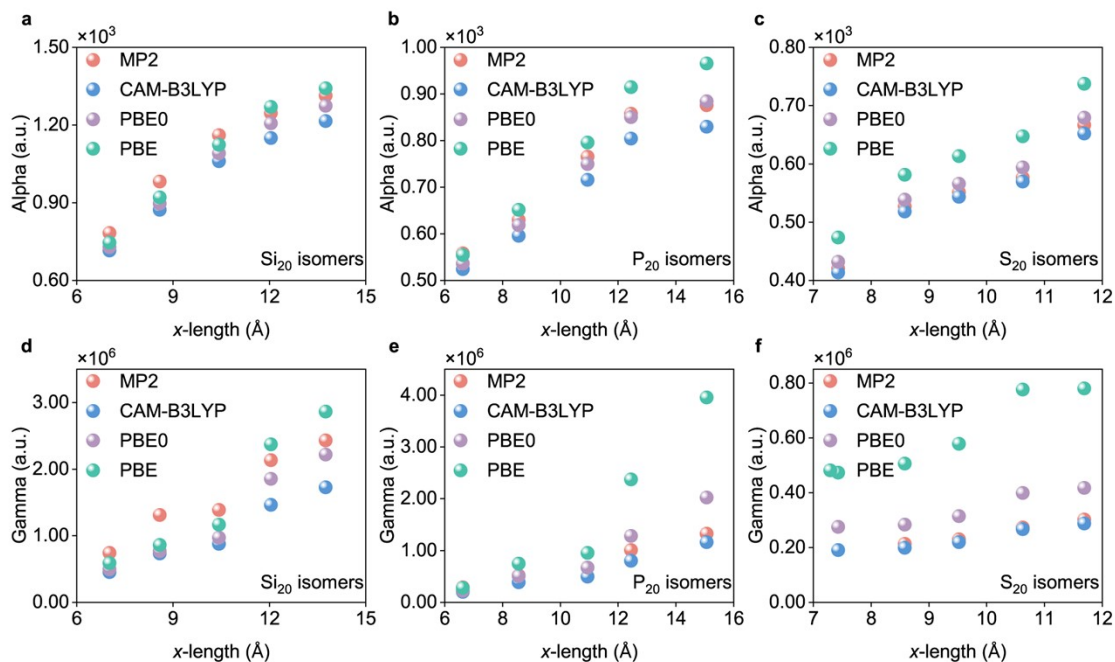


Figure S2. Assessments for calculating the linear and nonlinear optical responses of silicon, phosphorus, and sulfur isomers. a–c, α_{xx} for (a) silicon, (b) phosphorus, and (c) sulfur isomers. d–f, γ_{xxxx} for (d) silicon, (e) phosphorus, and (f) sulfur isomers.

Optical response behaviors of atomic-cluster isomers

For traditional nonlinear optical materials such as inorganic crystals and organic π -conjugated molecules, the correlations between the nonlinear optical coefficients and bandgap or HOMO–LUMO gap are described by the multi-level model.^{35,36} A large bandgap or HOMO–LUMO gap usually leads to a small nonlinear optical coefficient in materials. However, atomic clusters do not follow the general trends observed for traditional nonlinear optical materials. As shown in **Figure S3**, weak positive correlations exist between α_{xx} , γ_{xxxx} and HOMO–LUMO gap for silicon and phosphorus cluster isomers; weak negative correlation exists between α_{xx} and HOMO–LUMO gap for sulfur cluster isomers. Although there exists a moderate negative correlation between γ_{xxxx} and HOMO–LUMO gap for sulfur cluster isomers, with a correlation coefficient of -0.535 , guiding the design of nonlinear optical media through HOMO–LUMO gap is still of little practical value. For instance, the $S_{20}(I)$ cluster possesses smallest γ_{xxxx} value among all investigated S_{20} isomers, however, most isomers (92.67%) have larger HOMO–LUMO gap; the $S_{20}(II)$ cluster possesses largest γ_{xxxx} value, however, considerable number of isomers (22.00%) have smaller HOMO–LUMO gap.

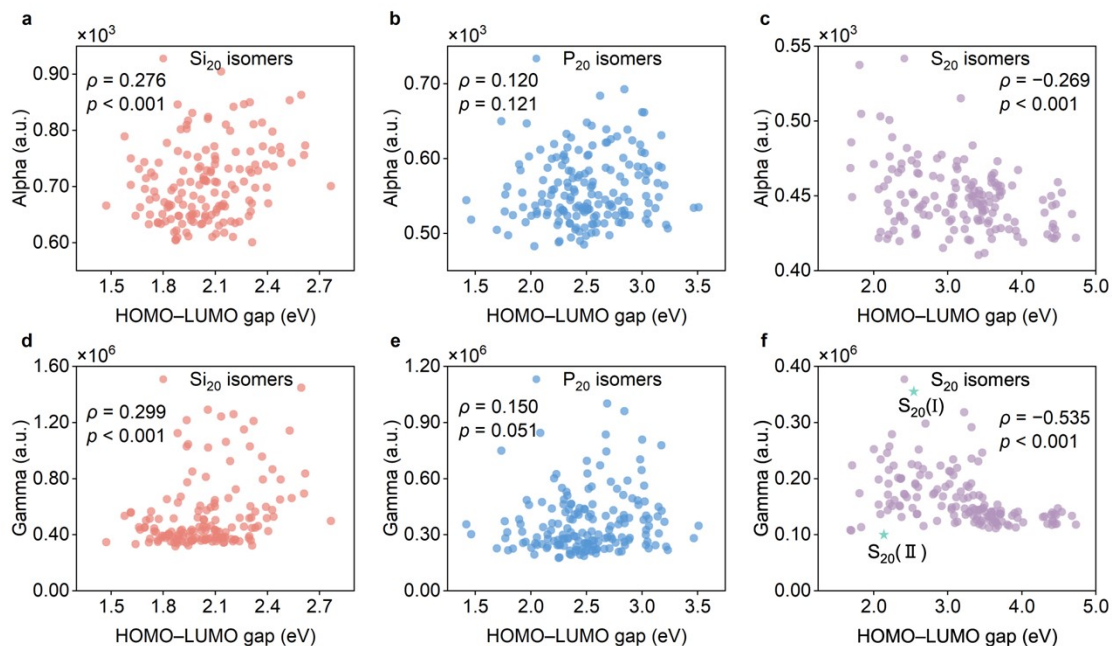


Figure S3. Measuring the linear and nonlinear optical responses of atomic clusters using the HOMO–LUMO gap descriptor. a–f, Correlations between α_{xx} , γ_{xxxx} and HOMO–LUMO gap for (a, d) silicon ($n = 151$), (b, e) phosphorus ($n = 169$), and (c, f) sulfur ($n = 150$) isomers. Correlations were assessed using Spearman (ρ) correlation coefficient. p refers to statistical significance.

For silicon, phosphorus, and sulfur cluster isomers, α_{ave} and γ_{ave} are significantly positively correlated with the maximum atomic distance. In fact, the correlations between α_{ave} , γ_{ave} and maximum atomic distance are better than the correlations between α_{ave} , γ_{ave} and x -length (**Figure S4**).

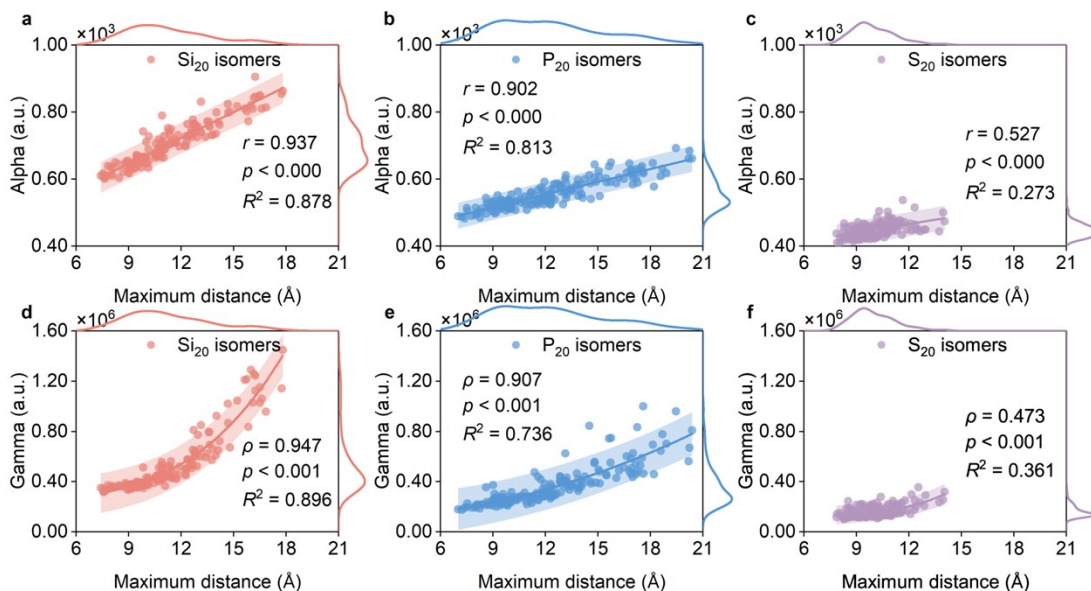


Figure S4. Measuring the linear and nonlinear optical responses of atomic clusters using the maximum atomic distance descriptor. a–c, Linear correlations between α_{ave} and maximum atomic distance and d–f exponential correlations between γ_{ave} and maximum atomic distance for (a, d) silicon ($n = 151$), (b, e) phosphorus ($n = 169$), and (c, f) sulfur ($n = 150$) isomers. Linear and exponential correlations were assessed using Pearson (r) and Spearman (ρ) correlation coefficients, respectively; p and R^2 represent statistical significance and the coefficient of determination of the fitting, respectively. Colored regions correspond to prediction bands with confidence level of 95%.

Optical response behaviors of 1D geometries

According to the method proposed above for assembling 1D silicon geometries, a Si_{20} isomer with x -length up to 21.46 Å is designed. Compared with other examined silicon-cluster isomers, the designed Si_{20} isomer exhibits the strongest linear and nonlinear optical responses, while occupying a large HOMO–LUMO gap (**Figure S5**).

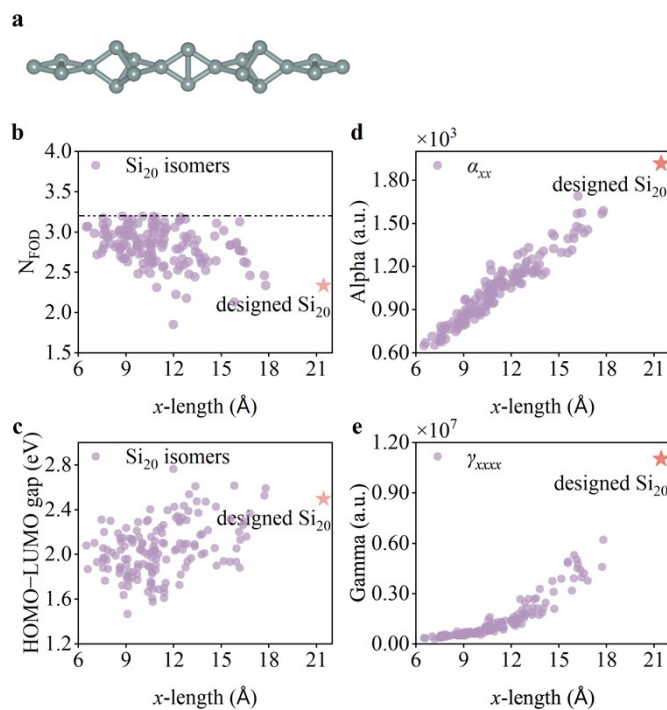


Figure S5. Optical responses of the designed Si_{20} isomer. (a) Geometry. (b) N_{FOD} . (c) HOMO–LUMO gap. (d) α_{xx} . (e) γ_{xxxx} .

Acetylene oligomers (*trans*-configuration), a classical 1D π -conjugated nonlinear optical molecules, are taken for comparison (**Figure S6**).

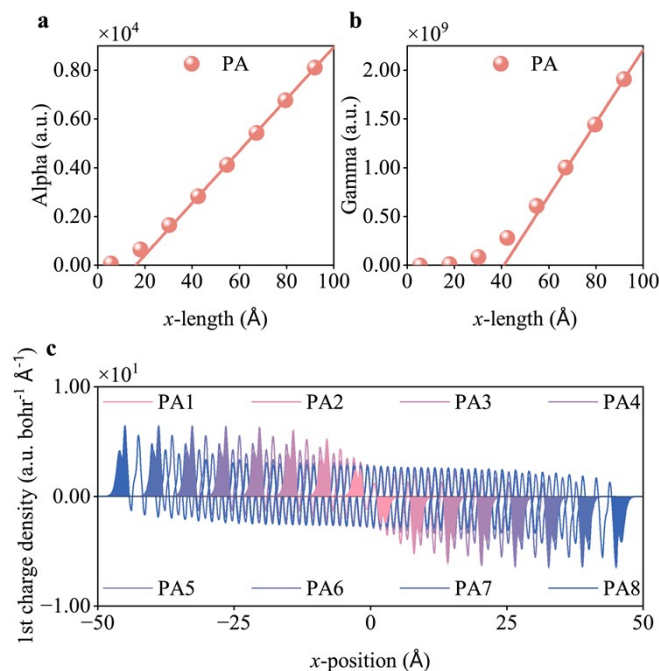


Figure S6. Optical responses of the acetylene oligomers (*trans*-configuration). (a) Dependence of α_{xx} on x -length. (b) Dependence of γ_{xxxx} on x -length. (c) 1st-order response-charge curves at various x -position. Coloured regions correspond to 1st-order external response charges.

References

- 1 C. Adamo and V. Barone, *J. Chem. Phys.*, 1999, **110**, 6158–6170.
- 2 M. Ernzerhof and G. E. Scuseria, *J. Chem. Phys.*, 1999, **110**, 5029–5036.
- 3 F. Weigend and R. Ahlrichs, *Phys. Chem. Chem. Phys.*, 2005, **7**, 3297–3305.
- 4 S. Grimme, J. Antony, S. Ehrlich and H. Krieg, *J. Chem. Phys.*, 2010, **132**, 154104.
- 5 S. Grimme, S. Ehrlich and L. Goerigk, *J. Comput. Chem.*, 2011, **32**, 1456–1465.
- 6 J. P. Perdew, K. Burke and M. Ernzerhof, *Phys. Rev. Lett.*, 1996, **77**, 3865–3868.
- 7 A. D. Becke, *J. Chem. Phys.*, 1993, **98**, 5648–5652.
- 8 P. J. Stephens, F. J. Devlin, C. F. Chabalowski and M. J. Frisch, *J. Phys. Chem.*, 1994, **98**, 11623–11627.
- 9 S. Grimme, *J. Chem. Phys.*, 2006, **124**, 034108.
- 10 T. N. Kitsopoulos, C. J. Chick, Y. Zhao and D. M. Neumark, *J. Chem. Phys.*, 1991, **95**, 1441–1448.
- 11 E. C. Honea, A. Ogura, C. A. Murray, K. Raghavachari, W. O. Sprenger, M. F. Jarrold and W. L. Brown, *Nature*, 1993, **366**, 42–44.
- 12 A. Fielicke, J. T. Lyon, M. Haertelt, G. Meijer, P. Claes, J. de Haeck and P. Lievens, *J. Chem. Phys.*, 2009, **131**, 171105.
- 13 A. Marijnissen and J. J. ter Meulen, *Chem. Phys. Lett.*, 1996, **263**, 803–810.
- 14 K. Fuke, K. Tsukamoto, F. Misaizu and M. Sanekata, *J. Chem. Phys.*, 1993, **99**, 7807–7812.
- 15 K. P. Huber, *Molecular Spectra and Molecular Structure: IV. Constants of Diatomic Molecules*, Springer Science & Business Media, 2013.
- 16 N. J. Brassington, H. G. M. Edwards and D. A. Long, *J. Raman Spectrosc.*, 1981, **11**, 346–348.
- 17 I. R. Beattie, G. A. Ozin and R. O. Perry, *J. Chem. Soc. A*, 1970, 2071–2074.
- 18 R. O. Jones, G. Ganteför, S. Hunsicker and P. Pieperhoff, *J. Chem. Phys.*, 1995, **103**, 9549–9562.

- 19 J. A. Zimmerman, S. B. H. Bach, C. H. Watson and J. R. Eyler, *J. Phys. Chem.*, 1991, **95**, 98–104.
- 20 S. Millefiori and A. Alparone, *J. Phys. Chem. A*, 2001, **105**, 9489–9497.
- 21 S. Hunsicker, R. O. Jones and G. Ganteför, *J. Chem. Phys.*, 1995, **102**, 5917–5936.
- 22 J. Berkowitz and C. Lifshitz, *J. Chem. Phys.*, 1968, **48**, 4346–4350.
- 23 S. Grimme and A. Hansen, *Angew. Chem.-Int. Edit.*, 2015, **54**, 12308–12313.
- 24 B. Champagne, E. A. Perpete, S. J. A. van Gisbergen, E.-J. Baerends, J. G. Snijders, C. Soubra-Ghaoui, K. A. Robins and B. Kirtman, *J. Chem. Phys.*, 1998, **109**, 10489–10498.
- 25 K. S. Kaka, P. Beaujean, F. Castet and B. Champagne, *J. Chem. Phys.*, 2023, **159**, 114104.
- 26 T. Yanai, D. P. Tew and N. C. Handy, *Chem. Phys. Lett.*, 2004, **393**, 51–57.
- 27 D. E. Woon and T. H. Dunning, *J. Chem. Phys.*, 1993, **98**, 1358–1371.
- 28 D. E. Bernholdt and R. J. Harrison, *Chem. Phys. Lett.*, 1996, **250**, 477–484.
- 29 F. Weigend, M. Häser, H. Patzelt and R. Ahlrichs, *Chem. Phys. Lett.*, 1998, **294**, 143–152.
- 30 M. Feyereisen, G. Fitzgerald and A. Komornicki, *Chem. Phys. Lett.*, 1993, **208**, 359–363.
- 31 F. Weigend and M. Häser, *Theor. Chem. Acc.*, 1997, **97**, 331–340.
- 32 F. Neese, F. Wennmohs, A. Hansen and U. Becker, *Chem. Phys.*, 2009, **356**, 98–109.
- 33 B. Helmich-Paris, B. de Souza, F. Neese and R. Izsák, *J. Chem. Phys.*, 2021, **155**, 104109.
- 34 S. Kossmann and F. Neese, *J. Chem. Theory Comput.*, 2010, **6**, 2325–2338.
- 35 M. G. Kuzyk, J. Perez-Moreno and S. Shafei, *Phys. Rep.*, 2013, **529**, 297–398.
- 36 R. Lytel, S. Mossman, E. Crowell and M. G. Kuzyk, *Phys. Rev. Lett.*, 2017, **119**, 073902.